# Multiwavelength spectral evolution during the 2011 outburst of the very faint X-ray transient Swift J1357.2-0933

Armas Padilla, M.; Degenaar, N.; Russell, D.M.; Wijnands, R.

*Published in:*
Monthly Notices of the Royal Astronomical Society

*DOI:*
10.1093/mnras/sts255

Monthly Notices
of the
ROYAL ASTRONOMICAL SOCIETY

MNRAS **428,** 3083–3088 (2013) doi:10.1093/mnras/sts255

# Multiwavelength spectral evolution during the 2011 outburst of the very faint X-ray transient Swift J1357.2−0933

M. Armas Padilla,[1★] N. Degenaar,[2] D. M. Russell[3] and R. Wijnands[1]

[1] *Astronomical Institute 'Anton Pannekoek', University of Amsterdam, Postbus 94249, 1090 GE Amsterdam, the Netherlands*
[2] *University of Michigan, Department of Astronomy, 500 Church Street, Ann Arbor, MI 48109, USA*
[3] *Instituto de Astrofísica de Canarias (IAC), Vía Láctea s/n, La Laguna 38205, S/C de Tenerife, Spain*

Accepted 2012 October 19. Received 2012 October 2; in original form 2012 July 16

## ABSTRACT

We report our multiwavelength study of the 2011 outburst evolution of the newly discovered black hole candidate X-ray binary Swift J1357.2−0933. We analysed the *Swift* X-ray Telescope and Ultraviolet/Optical Telescope (UVOT) data taken during the ∼7 months duration of the outburst. It displayed a 2–10 keV X-ray peak luminosity of $\sim 10^{35}$(D/1.5 kpc)$^2$ erg s$^{-1}$, which classifies the source as a very faint X-ray transient. We found that the X-ray spectrum at the peak was consistent with the source being in the hard state, but it softened with decreasing luminosity, a common behaviour of black holes returning to quiescence from the hard state. The correlations between the simultaneous X-ray and ultraviolet/optical data suggest a system with a black hole accreting from a viscous disc, and we do not detect X-ray reprocessing on the disc surface. The UVOT filters provide the opportunity to study these correlations up to ultraviolet wavelengths, a regime so far unexplored. If the black hole nature is confirmed, Swift J1357.2−0933 would be one of the very few established black hole very-faint X-ray transients.

**Key words:** accretion, accretion discs – stars: individual: Swift J1357.2–0933 – X-rays: binaries.



## 1 INTRODUCTION

X-ray binaries are the brightest X-ray point sources in our Galaxy. They are black holes (BHs) or neutron stars (NSs) accreting material from a companion star. The transient X-ray binaries alternate long epochs of quiescence during which they have X-ray luminosities of $L_X \sim 10^{30-33}$ erg s$^{-1}$ with outburst episodes during which the luminosity increases more than two orders of magnitude. The systems that reach a peak X-ray luminosity in their outbursts of only $L_X^{peak} \sim 10^{34-36}$ erg s$^{-1}$ are called *very faint* X-ray binary transients (VFXTs). They are several orders of magnitude fainter at their peaks than the better studied *faint* ($L_X^{peak} \sim 10^{36-37}$ erg s$^{-1}$) and *bright* ($L_X^{peak} \sim 10^{37-39}$ erg s$^{-1}$) systems (Wijnands et al. 2006).

It is in the last decade that VFXTs have been investigated in detail, thanks to the improvement in sensitivity and resolution of the X-ray instruments in orbit. However, even though the number of known sources has increased, their characteristics are still not well known. A considerable fraction of them have exhibited thermonuclear type I X-ray bursts, identifying the accretor as an NS (e.g. Cornelisse et al. 2002; Chelovekov & Grebenev 2007; Del Santo et al. 2007; Degenaar & Wijnands 2009).

Swift J1357.2−0933 is a new VFXT BH candidate (Casares et al. 2011; Corral-Santana et al., private communication) discovered with the *Swift* Burst Alert Telescope (BAT; Barthelmy et al. 2005) on 2011 January 28 (Krimm et al. 2011b). In the following days, it was observed with several X-ray satellites as well as ground-based telescopes. The MPI/ESO 2.2-m telescope at La Silla detected a new optical source within the *Swift*/BAT error circle. The magnitude difference compared to archival Sloan Digital Sky Survey (SDSS) images (when the source was in quiescence) was ∼6 mag. This indicates a Galactic origin, likely a low-mass X-ray binary (LMXB) or a dwarf nova outburst (Rau, Greiner & Filgas 2011), although the X-ray spectrum pointed to an LMXB nature (Krimm, Kennea & Holland 2011a). The SDSS photometry indicated that the quiescent counterpart was very red and that the companion was likely an M4 star. This resulted in a distance estimate of ∼1.5 kpc (Rau et al. 2011). In this work, we present analysis of the *Swift* X-ray and ultraviolet–optical (UV/optical) data of Swift J1357.2−0933 along its 2011 outburst.

## 2 OBSERVATIONS AND ANALYSIS

Immediately following its discovery, Swift J1357.2−0933 was monitored with the *Swift* satellite (Gehrels et al. 2004) throughout its outburst both with the X-ray Telescope (XRT; Burrows et al.

★ E-mail: m.armaspadilla@uva.nl


Published by Oxford University Press on behalf of the Royal Astronomical Society

**Table 1.** Log and XRT spectral results for Swift J1357.2−0933.

| ObsID | Date | Mode | Exp. time (ks) | Γ | $F_{\mathrm{X,\,abs}}$ [a] | $F_{\mathrm{X,\,unabs}}$ [a] | $L_X$ [b] | $\chi^2_\nu$/d.o.f. |
|---|---|---|---|---|---|---|---|---|
| 31918002 | 2/1/11 | WT | 3.28 | 1.53 ± 0.02 | 404 ± 6 | 408 ± 6 | 110 ± 2 | 0.98/323 |
| 31918003 | 2/2/11 | WT | 0.98 | 1.59 ± 0.03 | 374 ± 7 | 378 ± 7 | 102 ± 2 | 1.09/258 |
| 31918004 | 2/3/11 | WT | 1.63 | 1.56 ± 0.03 | 394 ± 7 | 398 ± 7 | 107 ± 2 | 0.95/263 |
| 31918005 | 2/4/11 | WT | 1.65 | 1.56 ± 0.02 | 365 ± 6 | 369 ± 5 | 99.4 ± 1.5 | 0.98/313 |
| 31918007 | 2/6/11 | WT | 1 | 1.54 ± 0.03 | 360 ± 7 | 364 ± 7 | 98.1 ± 1.8 | 0.96/250 |
| 31918008 | 2/7/11 | WT | 1.1 | 1.53 ± 0.03 | 341 ± 6 | 345 ± 6 | 92.9 ± 1.7 | 0.95/260 |
| 31918009 | 2/8/11 | WT | 1.74 | 1.52 ± 0.03 | 338 ± 6 | 342 ± 6 | 91.9 ± 1.6 | 1.10/274 |
| 31918010 | 2/9/11 | WT | 1.14 | 1.57 ± 0.03 | 321 ± 6 | 325 ± 6 | 87.5 ± 1.7 | 0.90/244 |
| 31918011 | 2/10/11 | WT | 1.03 | 1.55 ± 0.03 | 310 ± 6 | 314 ± 6 | 84.5 ± 1.7 | 1.08/240 |
| 31918012 | 2/11/11 | WT | 1.19 | 1.56 ± 0.03 | 303 ± 5 | 306 ± 5 | 82.5 ± 1.5 | 0.94/260 |
| 31918013 | 2/16/11 | WT | 1 | 1.53 ± 0.03 | 292 ± 6 | 296 ± 6 | 79.6 ± 1.7 | 0.99/224 |
| 31918014 | 2/18/11 | WT | 1.25 | 1.53 ± 0.03 | 258 ± 5 | 261 ± 5 | 70.2 ± 1.4 | 0.88/239 |
| 31918015 | 2/20/11 | WT | 1.08 | 1.53 ± 0.04 | 228 ± 5 | 230 ± 5 | 62.0 ± 1.4 | 0.88/189 |
| 31918016 | 2/24/11 | WT | 0.49 | 1.57 ± 0.06 | 203 ± 7 | 205 ± 7 | 55.2 ± 1.9 | 1.02/99 |
| 31918017 | 2/26/11 | WT | 1.11 | 1.61 ± 0.04 | 172 ± 4 | 175 ± 4 | 47.0 ± 1.1 | 0.92/173 |
| 31918018 | 2/28/11 | WT | 1.39 | 1.57 ± 0.04 | 168 ± 4 | 170 ± 4 | 45.7 ± 1.0 | 0.78/203 |
| 31918019 | 3/2/11 | WT | 1.35 | 1.56 ± 0.04 | 157 ± 4 | 159 ± 4 | 42.8 ± 1.0 | 0.92/185 |
| 31918020 | 3/4/11 | WT | 1.31 | 1.53 ± 0.04 | 147 ± 4 | 148 ± 4 | 40.0 ± 1.0 | 1.02/174 |
| 31918021 | 3/6/11 | WT | 1.31 | 1.57 ± 0.04 | 130 ± 4 | 131 ± 4 | 35.4 ± 1.0 | 0.94/141 |
| 31918022 | 3/8/11 | WT | 1.3 | 1.52 ± 0.04 | 144 ± 4 | 145 ± 4 | 39.1 ± 1.0 | 0.97/160 |
| 31918023 | 3/10/11 | WT | 1.2 | 1.55 ± 0.04 | 123 ± 3 | 125 ± 3 | 33.6 ± 0.9 | 0.81/131 |
| 31918024 | 3/12/11 | WT | 1.38 | 1.57 ± 0.05 | 130 ± 4 | 132 ± 4 | 35.4 ± 1.0 | 1.12/114 |
| 31918025 | 3/13/11 | WT | 1.23 | 1.58 ± 0.05 | 106 ± 3 | 107 ± 3 | 28.8 ± 0.9 | 1.21/122 |
| 31918026 | 3/16/11 | WT | 0.25 | 1.53 ± 0.13 | 80.3 ± 6.6 | 81.2 ± 6.5 | 21.9 ± 1.7 | 0.97/22 |
| 31918027 | 3/18/11 | WT | 1.21 | 1.6 ± 0.05 | 85.3 ± 2.8 | 86.3 ± 2.8 | 23.2 ± 0.8 | 0.97/102 |
| 31918028 | 3/20/11 | WT | 1.22 | 1.52 ± 0.1 | 97.5 ± 5.8 | 98.5 ± 5.8 | 26.5 ± 1.6 | 0.88/45 |
| 31918029 | 3/29/11 | WT | 1.27 | 1.57 ± 0.06 | 76.9 ± 3.1 | 77.8 ± 3.1 | 20.9 ± 0.8 | 0.97/76 |
| 31918030 | 4/3/11 | WT | 1.45 | 1.61 ± 0.06 | 63.6 ± 2.2 | 64.3 ± 2.2 | 17.3 ± 0.6 | 0.95/93 |
| 31918031 | 4/13/11 | WT | 1.34 | 1.47 ± 0.12 | 45.0 ± 3.2 | 45.4 ± 3.2 | 12.2 ± 0.8 | 0.53/29 |
| 31918032 | 4/20/11 | WT | 1.56 | 1.63 ± 0.08 | 36.2 ± 1.6 | 36.6 ± 1.6 | 9.87 ± 0.43 | 1.02/60 |
| 31918033 | 4/23/11 | WT | 1.26 | 1.6 ± 0.09 | 35.4 ± 1.8 | 35.8 ± 1.8 | 9.63 ± 0.49 | 0.84/49 |
| 31918034 | 4/28/11 | WT | 1.24 | 1.73 ± 0.15 | 19.9 ± 1.7 | 20.2 ± 1.7 | 5.45 ± 0.46 | 1.10/26 |
| 31918035 | 5/3/11 | WT | 1.12 | 1.79 ± 0.1 | 28.3 ± 1.7 | 28.7 ± 1.6 | 7.73 ± 0.44 | 1.00/38 |
| 31918036 | 5/8/11 | WT | 1.02 | 1.72 ± 0.13 | 21.9 ± 1.6 | 22.2 ± 1.6 | 5.97 ± 0.43 | 1.04/25 |
| 31918037 | 5/13/11 | WT | 1.34 | 1.69 ± 0.13 | 21.5 ± 1.6 | 21.8 ± 1.6 | 5.87 ± 0.44 | 1.08/21 |
| 31918038 | 6/15/11 | PC | 1.15 | 1.87 ± 0.25 | 5.64 ± 0.70 | 5.74 ± 0.69 | 1.54 ± 0.19 | 0.95/31 |
| 31918039 | 6/29/11 | PC | 1.24 | 1.89 ± 0.27 | 3.92 ± 0.51 | 3.99 ± 0.50 | 1.07 ± 0.13 | 0.99/23 |
| 31918040 | 7/14/11 | PC | 1.07 | 1.76 ± 0.53 | 3.23 ± 0.85 | 3.28 ± 0.84 | 0.88 ± 0.23 | 1.00/10 |
| 31918041 | 7/28/11 | PC | 0.65 | $2.13^{+1.86}_{-0.95}$ | 1.65 ± 0.81 | 1.69 ± 0.79 | 0.45 ± 0.21 | 1.21/4 |
| 31918043 | 8/23/11 | PC | 1.19 | 2.13 (fix) | <0.22 | <0.23 | <0.06 | – |
| 31918044 | 9/5/11 | PC | 2.05 | 2.13 (fix) | <0.07 | <0.08 | <0.02 | – |

*Note*. $N_{\mathrm{H}}$ has been fixed to $1.2 \times 10^{20}$ cm$^{-2}$, value inferred from the high-resolution X-ray spectra obtained with *XMM–Newton* (Armas Padilla et al., in preparation), which is consistent with that reported by Krimm et al. (2011a).
[a]Flux in units of $10^{-12}$ erg cm$^{-2}$ s$^{-1}$ in the 0.5–10 keV energy band.
[b]X-ray luminosity in units of $10^{33}$ erg s$^{-1}$ calculated from the 0.5–10 keV unabsorbed flux by adopting a distance of 1.5 kpc.

2005) and the Ultraviolet/Optical Telescope (UVOT; Roming et al. 2005), which lasted ∼7 months. A total of 42 pointings were performed during this period, for a total exposure time of 54.8 ks. A log of the observations is given in Table 1. The observations were performed daily in the first 10 d, and once every 2 d in the following month. After that, the observations were separated by one to two weeks.

### 2.1 XRT data

The *Swift*/XRT observations were obtained both in photon counting (PC) and windowed timing (WT) modes. Due to the high flux of Swift J1357.2−0933, the XRT was operated in WT mode in the early observations in order to avoid pile-up (except for the first observation; see below). When the count rate was below 0.5 count s$^{-1}$, the observations were taken in PC mode (see Table 1). The data were processed using the HEASOFT v.6.11 software. The raw data were reduced running the `xrtpipeline` task in which standard event grades of 0–12 were selected for the PC data and 0–2 for the WT mode observations.

For every observation, spectra, light curves and images were obtained using `Xselect`. The regions to extract the source events for both PC and WT modes were centred at the source position (RA = $13^{\mathrm{h}}57^{\mathrm{m}}16\overset{\mathrm{s}}{.}86$, Dec. = $-09°32'38\overset{''}{.}9$, J2000, 0.42 arcsec error radius; Krimm et al. 2011a). For the WT data, we used a circle of ∼27 pixels radius for the source, and for the background extraction we used an annulus centred on the source with ∼64 pixels for the inner radius and ∼118 pixels for the outer radius. In the case of the PC mode observations, the region used was a circle of ∼10 pixels radius for the source, and for the background three circular regions with the same size located in nearby source-free regions.

To look for eclipses, dips or X-ray bursts, we checked the light curves with different bin sizes extracted for each observation. We did not detect any evidence or feature that suggests modulations or a pattern in the source flux, although we cannot rule out with high confidence the presence of any modulations due to the low count rate. We created the exposure maps in order to correct for the effect of bad columns on the CCD, which in turn are used to create the ancillary response files using the `xrtmkarf` task. The latest versions of the response matrix files (v.14) were taken from the HEASARC calibration data base. Finally, with `grppha` we grouped the spectra to have a minimum of 20 photons per bin to be able to consistently use the $\chi^2$. Due to the low number of counts collected during observations 38–41,[1] we fitted these data using both *C*-statistic and $\chi^2$ but grouped them with a minimum of five photons per bin. The results using both methods were consistent with each other.

The first observation 01 was taken in PC mode, which is severely affected by pile-up. It has a count rate of 2.3 count $s^{-1}$, while the pile-up becomes considerable in PC mode for count rates above ~0.6 count $s^{-1}$ (Evans et al. 2009; see also the *Swift*/XRT analysis web[2]). Therefore, we do not include this observation in our analysis. In the last two XRT observations (43 and 44), the source was not detected. The count rates were calculated using the prescription for small numbers of counts given by Gehrels (1986). We calculated the 95 per cent confidence upper limits on the flux with WebPIMMS HEASARC tool.[3] An absorbed power-law model with a hydrogen column density ($N_{\rm H}$) of $1.2 \times 10^{20}$ cm$^{-2}$ (see Section 3) was assumed. We used a photon index of $\Gamma = 2.13$, which corresponds to the value we obtained in the last observation where the source was detected.

In order to improve the statistics, we have also combined observations that were performed within a few days time span and that yielded comparable fluxes. As such, we have combined observations 03–05, 07–12, 13–15, 17–20, 21–25, 26–20, 30–33, 34–37, 38–41 and 43–44. We extracted the combined spectra, light curves and images in the same way as the individual cases. We merged the individual exposure maps created for each image using the task `ximage`.

### 2.2 UVOT data

The UVOT observations were performed in image mode. Most of them were taken with six filters (*v*, *b*, *u*, *uvw*1, *uvm*2, *uvw*2) but some of them with only a few filters and sometimes only one. We calculated the source's magnitude (in the Vega system) and flux densities with the `uvotsource` tool, which performs aperture photometry on the sky images. We selected a circular region with a radius of 5 arcsec centred on the source and a circular source-free region with a radius of 18 arcsec for the background correction. We corrected the magnitudes and fluxes for the Galactic extinction. The reddening is $E(B-V) = 0.04$ mag in the direction of Swift J1357.2−0933 (Schlegel, Finkbeiner & Davis 1998). Using this value and the prescription of Pei (1992), we calculate the extinction for every band. The obtained values are $A_v = 0.123$, $A_b = 0.163$, $A_u = 0.193$, $A_{uvw1} = 0.263$, $A_{uvm2} = 0.387$ and $A_{uvw2} = 0.349$. The source is located at high Galactic latitude ($b = 50.0042$), and for a distance of 1.5 kpc or larger, the source will be located outside the plane of the Galaxy. Therefore, the measured column density (or reddening) corresponds to the full Galactic one in that direction. In the case of no source detection, the `uvotsource` tool returns a $3\sigma$ upper limit for the magnitudes.

[1] We refer to the observations with the last two numbers of their observation IDs in the main text. The full observation IDs are in Table 1.

[2] http://www.swift.ac.uk/analysis/xrt/xselect.php.

[3] Available at http://heasarc.gsfc.nasa.gov/Tools/w3pimms.html.

## 3 RESULTS

### 3.1 X-ray light curve and spectra

We fitted the spectra using XSPEC (v.12.7.0). All observations were well fitted with a simple power law (`powerlaw`) affected by photoelectric absorption (`phabs`). We assumed a column density to Swift J1357.2−0933 of $1.2 \times 10^{20}$ cm$^{-2}$ constant with time. We inferred this value from the high-resolution X-ray spectra obtained with *XMM–Newton* (Armas Padilla et al., in preparation), which is consistent with that reported by Krimm et al. (2011a). The results are reported in Table 1, where the flux errors have been calculated following the procedure presented in Wijnands et al. (2004). We also tried other single-component models like a blackbody (`bbodyrad`) and an accretion disc consisting of multiple blackbody components (`diskbb`; Makishima et al. 1986) but both models could not fit the data accurately ($\chi^2_\nu > 3$ and $\chi^2_\nu > 1.5$, respectively). A two-component model (`diskbb+powerlaw`) can fit the data as well; however, it does not improve the best fit of the single power-law model and the additional thermal component contributes only a few per cent of the total flux.

In Fig. 1, we show the 0.5–10 keV light curve. The outburst has its maximum as observed during observation 02 in the beginning,[4] where the peak of the unabsorbed flux is $4.1 \times 10^{-10}$ erg cm$^{-2}$ s$^{-1}$. This corresponds to a peak luminosity of $1.1 \times 10^{35}$ erg s$^{-1}$ assuming a distance of 1.5 kpc (Rau et al. 2011). After this, the luminosity monotonically decreases until the source goes undetected using the XRT ~180 d after the discovery date. The upper limits on the luminosity calculated from the last two observations are between 2 and $6 \times 10^{31}$ erg s$^{-1}$.

Plotting the photon index evolution with time (Fig. 1) shows that the photon index increases from a value of $\Gamma \sim 1.5$ to a value of $\Gamma \sim 2$, indicating that the spectra became softer during the decay of the outburst. This softening behaviour is also seen when using the hardness ratio (HR; Fig. 1, left-hand panel). The HR is defined as the ratio between the counts in the hard band (2–10 keV) and the counts in the soft band (0.5–2 keV). We have performed the same analysis when combining sets of observations (see Section 2.1). The result is shown in Fig. 1 (right-hand panel). Due to the smaller error bars, the increase of the photon index and the HR decay are more clearly visible.

### 3.2 Ultraviolet/optical and X-ray correlation

The *Swift*/UVOT observations were taken simultaneously with the X-ray ones. Most of the observations were taken with all six filters, which allows us to study the correlation between the X-ray and the UV/optical emission along the outburst. Fig. 2 shows the X-ray light curve and the UV/optical magnitudes in the Vega system. The last UVOT detection (*u* band) was 203 d after the first detection when the source was already undetected in X-ray. Over the course of the outburst, the brightness in all bands is decreasing simultaneously

[4] Observation 01 could be brighter, but due to the strong pile-up it was not included in the analysis.

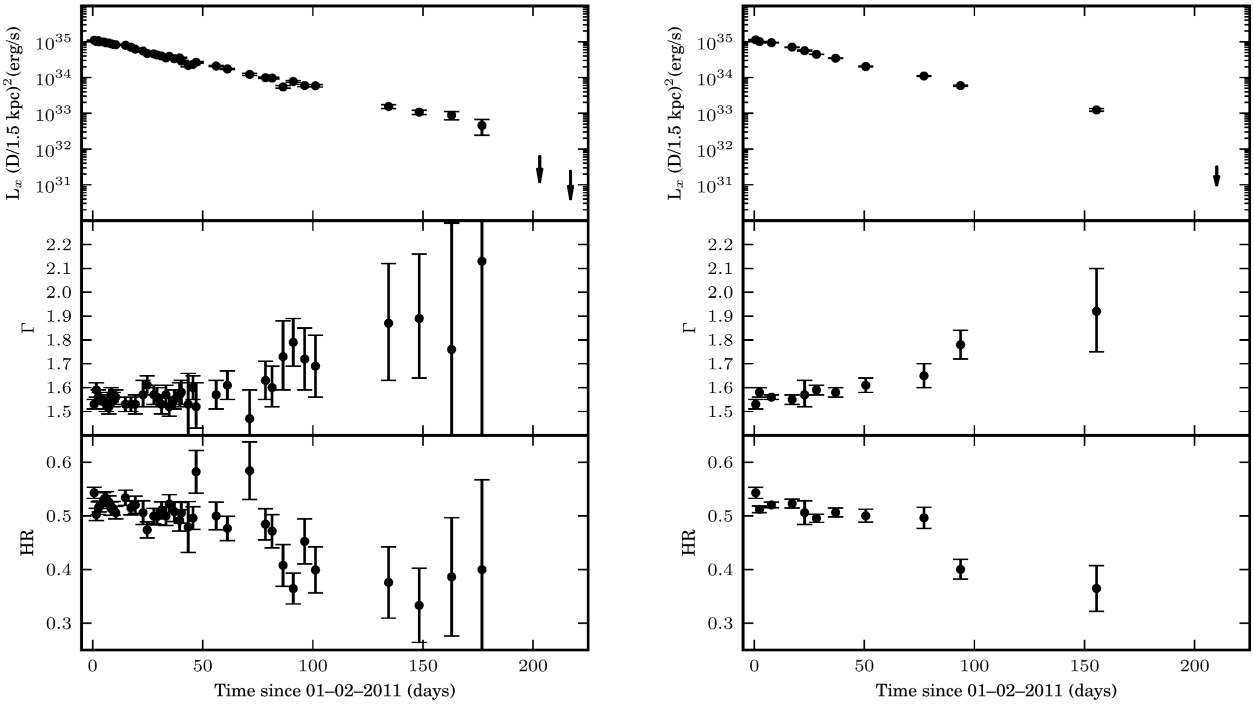


**Figure 1.** In both plots, the upper panel is the light curve (0.5–10 keV; assumed distance of 1.5 kpc), the central panel is the photon index evolution with time and the bottom panel is the hardness ratio evolution with time (ratio of the counts in the hard, 2–10 keV, and soft, 0.5–2 keV, energy bands). All data are plotted in the left-hand panel, whereas in the right-hand panel we present the result of the combined sets of observations (see Section 2.1).

with the decline in the X-rays. This resulted in a clear correlation between X-ray and UV/optical fluxes, which is shown in Fig. 3. We have assumed a power-law model to fit these correlations and calculate the correlation slopes $\beta$ ($F_{\rm UV/optical} \propto F_{\rm X}^{\beta}$). We have calculated $\beta$ for every UVOT band and for the X-ray flux in the 2–10 keV energy range in order to compare them with values in previous publications (e.g. Russell et al. 2006). However, the spectral resolution of *Swift*/XRT allows us to also measure the correlation slopes for X-ray fluxes in the 0.5–10 keV energy range. The results are shown in Table 2. Clearly, $\beta$ increases towards shorter wavelengths, going from 0.2 in the *v* band to 0.37 in the *uvw*2 band (using the 0.5–10 keV energy range). The numbers become 0.19–0.35 in the 2–10 keV range (see Fig. 4).

## 4 DISCUSSION

We have analysed the XRT and UVOT data taken over the ∼7 months duration of the 2011 outburst of the newly discovered candidate BH LMXB Swift J1357.2−0933. We fitted the *Swift*/XRT spectra using a simple power-law model affected by absorption. The peak flux was reached at the beginning of the outburst, after which it steadily decreased until the source went undetected with XRT ∼180 d after its discovery. The unabsorbed peak flux has a value of $F_{\rm X,\,unabs} = 4.1 \times 10^{-10}$ erg cm$^{-2}$ s$^{-1}$ in the 0.5–10 keV energy range, which corresponds to an outburst peak luminosity of $L_{\rm X} = 1.1 \times 10^{35}$ erg s$^{-1}$ assuming a distance of 1.5 kpc. This low peak luminosity classifies Swift J1357.2−0933 as a VFXT, which has peak luminosities $L_{\rm X}^{\rm peak} < 10^{36}$ erg s$^{-1}$. Even if the source was located at a distance of 8 kpc, the inferred peak luminosity is a few times $10^{36}$ erg s$^{-1}$, still in the faint regime. However, such long distance is unlikely since the high Galactic latitude ($b = 50.0042$) would place Swift J1357.2−0933 at 6 kpc above the Galactic plane.

The system was in the hard state at peak of the outburst and remained in this state throughout the outburst, which is usual at these low X-ray luminosities (see Belloni 2010, for the state definitions). From the first observation until the last one, the spectral index of the power law increases from 1.5 to 2.1. As can be seen in Fig. 1, the X-ray luminosity and photon index are anticorrelated. The softening can also be seen in the HR curve demonstrating that it does not depend on assumed spectral model. It shows how the spectrum becomes softer as the luminosity decays (Fig. 1). Such softening behaviour was also present in the VFXT XTE J1719−291 (Armas Padilla et al. 2011), but for this source the spectra were considerably softer, with a photon index regime from $\Gamma = 2.0$ to 2.7. The reason for Swift J1357.2−0933 to have harder spectra than XTE J1719−291 could be a difference in the nature of their compact objects. Although it is not established, the characteristics of XTE J1719−291 favour an NS accretor (Armas Padilla et al. 2011), whereas Swift J1357.2−0933 has been identify as a strong BH candidate system using optical spectroscopy (Casares et al. 2011, Corral-Santana et al., private communication).

The upper limit on the luminosity inferred from the non-detections in the last two observations is $L_{\rm X} \sim 2 \times 10^{31}$ erg s$^{-1}$. This could indicate that the nature of the accretor is a BH since they typically have quiescent luminosities in the range of $L_{\rm X} \sim 10^{30}$–$10^{31}$ erg s$^{-1}$, while the NSs usually have quiescent luminosities $L_{\rm X} > 10^{32}$ erg s$^{-1}$ (but see Jonker et al. 2007, for an exception).

Several other BH sources have shown softening in their X-ray spectra at low luminosities. XTE J1650−500 softened in its 2001–2002 outburst. The photon index changed from $\Gamma = 1.66$ to 1.93 when the luminosity decayed to $2 \times 10^{34}$ erg s$^{-1}$ (Tomsick, Kalemci & Kaaret 2004). Also, at these intermediate luminosities, 4U 1543−47 evolved from a photon index of $\Gamma = 1.64$ in its hard state to a photon index of $\Gamma = 2.22$ at lower $L_{\rm X}$ (Kalemci et al. 2005). By studying a sample of seven BHs in their quiescence state,

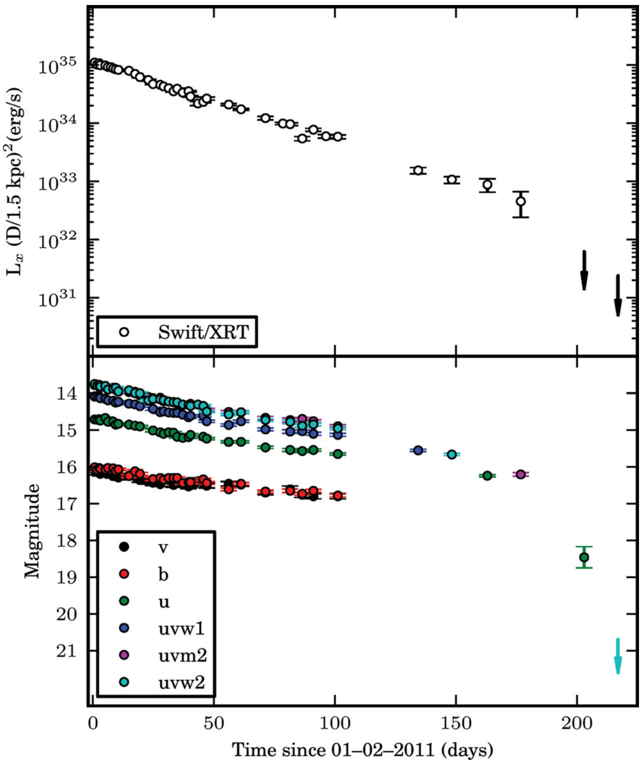


**Figure 2.** In the top panel, the X-ray light curve in the 0.5–10 keV energy band for a distance of 1.5 kpc is shown, while in the bottom panel the UV/optical light curves in the Vega system are plotted.

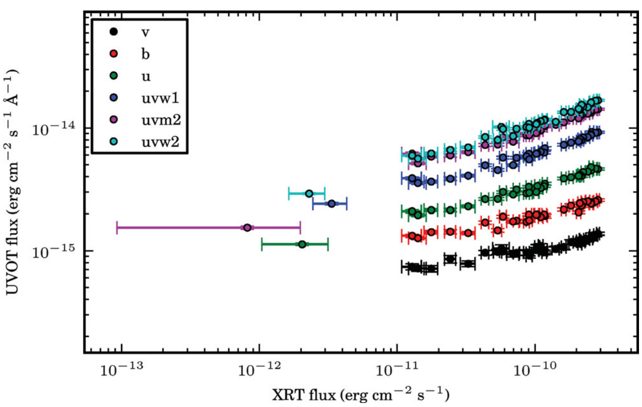


**Figure 3.** Correlation between the UV/optical density fluxes and the X-ray 2–10 keV flux.

**Table 2.** Correlation slope between UV/optical and X-ray fluxes ($F_{\mathrm{UV/optical}} \propto F_{\mathrm{X}}{}^{\beta}$). $\lambda_{\mathrm{eff}}$ is the effective wavelength for each band.

| UVOT/band | $\lambda_{\mathrm{eff}}$ (Å) | $\beta$ 0.5–10 KeV | 2–10 keV |
|---|---|---|---|
| *v* | 5402 | 0.203 ± 0.019 | 0.199 ± 0.017 |
| *b* | 4329 | 0.237 ± 0.011 | 0.232 ± 0.011 |
| *u* | 3501 | 0.293 ± 0.007 | 0.286 ± 0.006 |
| *uvw*1 | 2634 | 0.321 ± 0.007 | 0.311 ± 0.006 |
| *uvm*2 | 2231 | 0.374 ± 0.007 | 0.357 ± 0.006 |
| *uvw*2 | 2030 | 0.370 ± 0.006 | 0.358 ± 0.005 |

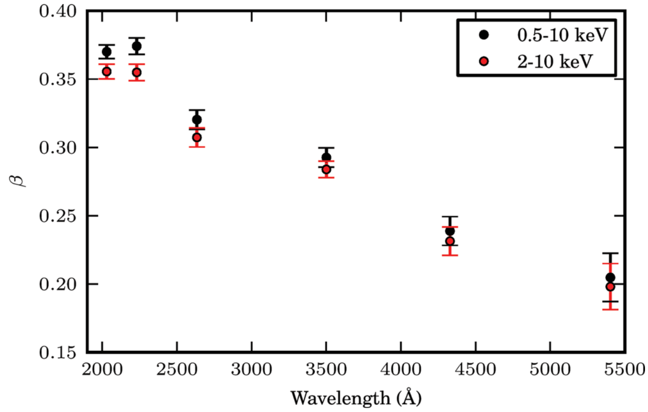


**Figure 4.** Correlation slopes ($\beta$) between the UVOT bands and the X-ray flux in the 0.5–10 keV and 2–10 keV energy bands.

Corbel, Tomsick & Kaaret (2006) arrived to the conclusion that all BHs are softer in quiescence than in the standard hard state. Using a study of 25 BHs, Dunn et al. (2010) presented data from which the same conclusion can be inferred: when data are available, the sources show softening towards quiescence. However, in the 2008 outburst decay of H 1743−322 to quiescence, Jonker et al. (2010) did not see any evidence of softening, although it cannot be ruled out that this is caused by the inaccuracy in the photon index due to the high $N_{\mathrm{H}}$.

### 4.1 X-ray and UV/optical simultaneous data: a non-irradiated accretion disc

The proximity and the low Galactic extinction towards Swift J1357.2−0933 have made it possible to obtain X-ray and UV/optical data simultaneously using XRT and UVOT instruments on-board *Swift*. Until today, this had not been possible for any VFXT since, in addition to their low luminosity, the vast majority are located towards the Galactic Centre, which makes it very difficult to detect the optical counterpart due to the high Galactic absorption.

The optical/UV and X-ray fluxes are strongly correlated during the outburst (Fig. 2). Russell et al. (2006) quantified the disc and jet contribution from the optical/infrared and X-ray (2–10 keV) correlation in the hard state. Based on the values of $\beta$ expected from the different emission processes (sections 3.3 and 3.4 of their work), our correlation in the *v* band is consistent with a BH accreting via a non-irradiated viscous disc. For a viscously heated disc, $0.15 \leq \beta \leq 0.25$ is expected in the case of a BH (for *V*-band optical and 2–10 keV X-ray), and for Swift J1357.2−0933 we find $\beta = 0.2$ (Table 2). For an NS, $0.3 \leq \beta \leq 0.5$ is predicted, so our correlation is consistent with optical emission from a viscously heated disc around a BH accretor. Higher values of $\beta$ are expected if the optical emission originates in an irradiated accretion disc or a jet.

Additionally, Frank, King & Raine (2002) predict a dependency of the slopes $\beta$ with the wavelength. For optical emission from a viscously heated steady-state disc, $\beta$ increases at shorter wavelengths. This is consistent with our results, where $\beta$ increases from 0.2 in the *v* band to 0.35 in the *uvw*2 one (see Table 2). Therefore, all the evidence favours UV/optical emission dominated by the viscously heated disc, with little or no X-ray irradiation detected.

## ACKNOWLEDGMENTS

MAP acknowledges J. Corral-Santanta and J. Casares for useful discussion on the nature of the source. MAP and RW are supported by a European Research Council Starting Grant awarded by RW. RW also acknowledges support from The European Community's Seventh Framework Programme (FP7/2007-2013) under grant agreement number ITN 215212 Black Hole Universe. ND is supported by NASA through Hubble Postdoctoral Fellowship grant number HST-HF-51287.01-A from the Space Telescope Science Institute (STScI). DMR is supported by a Marie Curie Intra European Fellowship within the 7th European Community Framework Programme under contract No. IEF 274805.


## REFERENCES


Armas Padilla M., Degenaar N., Patruno A., Russell D. M., Linares M., Maccarone T. J., Homan J., Wijnands R., 2011, MNRAS, 417, 659
Barthelmy S. D. et al., 2005, Space Sci. Rev., 120, 143
Belloni T. M., ed., 2010, Lecture Notes Phys. Vol. 794, The Jet Paradigm. Springer-Verlag, Berlin, p. 53
Burrows D. N. et al., 2005, Space Sci. Rev., 120, 165
Casares J., Torres M. A. P., Negueruela I., Gonzalez-Fernandez C., Corral-Santana J. M., Zurita C., Llano S. R., 2011, Astron. Telegram, 3206, 1
Chelovekov I. V., Grebenev S. A., 2007, Astron. Lett., 33, 807
Corbel S., Tomsick J. A., Kaaret P., 2006, ApJ, 636, 971
Cornelisse R. et al., 2002, A&A, 392, 885
Degenaar N., Wijnands R., 2009, A&A, 495, 547
Del Santo M., Sidoli L., Mereghetti S., Bazzano A., Tarana A., Ubertini P., 2007, A&A, 468, L17
Dunn R. J. H., Fender R. P., Körding E. G., Belloni T., Cabanac C., 2010, MNRAS, 403, 61
Evans P. A. et al., 2009, MNRAS, 397, 1177
Frank J., King A., Raine D. J., 2002, Accretion Power in Astrophysics, 3rd edn. Cambridge Univ. Press, Cambridge
Gehrels N., 1986, ApJ, 303, 336
Gehrels N. et al., 2004, ApJ, 611, 1005
Jonker P. G., Steeghs D., Chakrabarty D., Juett A. M., 2007, ApJ, 665, L147
Jonker P. G. et al., 2010, MNRAS, 401, 1255
Kalemci E., Tomsick J. A., Buxton M. M., Rothschild R. E., Pottschmidt K., Corbel S., Brocksopp C., Kaaret P., 2005, ApJ, 622, 508
Krimm H. A., Kennea J. A., Holland S. T., 2011a, Astron. Telegram, 3142, 1
Krimm H. A. et al., 2011b, Astron. Telegram, 3138, 1
Makishima K., Maejima Y., Mitsuda K., Bradt H. V., Remillard R. A., Tuohy I. R., Hoshi R., Nakagawa M., 1986, ApJ, 308, 635
Pei Y. C., 1992, ApJ, 395, 130
Rau A., Greiner J., Filgas R., 2011, Astron. Telegram, 3140, 1
Roming P. W. A. et al., 2005, Space Sci. Rev., 120, 95
Russell D. M., Fender R. P., Hynes R. I., Brocksopp C., Homan J., Jonker P. G., Buxton M. M., 2006, MNRAS, 371, 1334
Schlegel D. J., Finkbeiner D. P., Davis M., 1998, ApJ, 500, 525
Tomsick J. A., Kalemci E., Kaaret P., 2004, ApJ, 601, 439
Wijnands R., Homan J., Miller J. M., Lewin W. H. G., 2004, ApJ, 606, L61
Wijnands R. et al., 2006, A&A, 449, 1117


This paper has been typeset from a TEX/LATEX file prepared by the author.